CHAPTER 182

Littoral Transport Rate

J. William Kamphuis[1] M. ASCE

Abstract

This paper describes a study of littoral sediment transport rate based on three-dimensional hydraulic model experiments performed with regular and irregular waves. Deep water wave conditions, wave heights through the surf zone, wave breaking angles, longshore current velocity distribution and the bed load and suspended load sediment transport distributions were measured simultaneously to form a coherent data set. An expression is developed linking sediment transport rate to wave steepness, beach slope, relative grain size and breaking angle. The expression compares well with published field data.

1. Introduction

This paper describes the continuation of research on alongshore sediment transport described in Kamphuis and Readshaw (1978), Kamphuis and Sayao (1980) and Kamphuis et al. (1986). A new set of three dimensional mobile bed hydraulic beach model results is used; a summary of the tests is shown in Table 1; the experimental layout is shown in Figure 1 and more detail about the tests may be found in Kamphuis and Kooistra (1990).

2. General Description of the Tests

The section of the wave basin used was 23.4 m long by 10.0 m wide. An initial plane sand beach slope of 1:10 was prepared for each test. The depth of water in Table 1 was measured at the toe of the sloping beach.

Constant regular and irregular wave climates were generated for approximately 7 hours; the irregular waves consisted of a Jonswap spectrum with $\gamma = 2.3$ and the random wave signal typically repeated itself after 200

---

[1]Professor, Queen's University, Department of Civil Engineering, Kingston, Ontario K7L 3N6 CANADA

TABLE 1

SUMMARY OF 3-0 TESTS

Test	Generated Wave Hs (m)	Tp (sec)	d (m)	Wave Type	Groupiness Factor	Incident Angle	Grain Size 0 (mm)
IA	.045	1.15	.50	irr	.8	10	.105
IB	.063	1.15	.55	irr	.8	10	.18
IG	.088	1.15	.55	irr	.8	10	.18
IO	.117	1.15	.55	irr	.8	10	.18
IE	.063	0.92	.50	irr	.8	10	.105
IF	.063	1.15	.50	irr	.8	10	.105
IG	.063	1.39	.50	irr	.8	10	.105
II	.078	1.38	.50	irr	.8	10	.105
IJ	.090	0.92	.55	irr	.8	10	.18
IK	.084	1.38	.55	irr	.8	10	.18
IL	.122	1.15	.55	irr	.8	20	.18
IM	.094	1.15	.55	irr	.8	20	.18
IN	.063	1.15	.55	irr	.8	20	.18
IO	.063	1.15	.55	irr	.8	30	.18
*IP	.080	1.15	.55	irr	.8	30	.18
*IQ	.124	1.15	.55	irr	.8	30	.18
*IR	.084	1.15	.55	irr	.2	30	.18
*IS	.084	1.15	.55	irr	1.4	30	.18
*IT	.127	1.00	.55	irr	.8	40	.18
*IU	.139	1.50	.55	irr	.8	40	.18
*IV	.094	1.20	.55	irr	.8	40	.18
RG	.074	1.15	.55	reg		10	.18
RE	.045	0.92	.50	reg		10	.105
RG	.045	1.39	.50	reg		10	.105
RI	.060	1.38	.50	reg		10	.105
RM	.084	1.15	.55	reg		20	.18
*RP	.051	1.15	.55	reg		30	.18
RT	.132	1.00	.55	reg		40	.18

* VIOEO

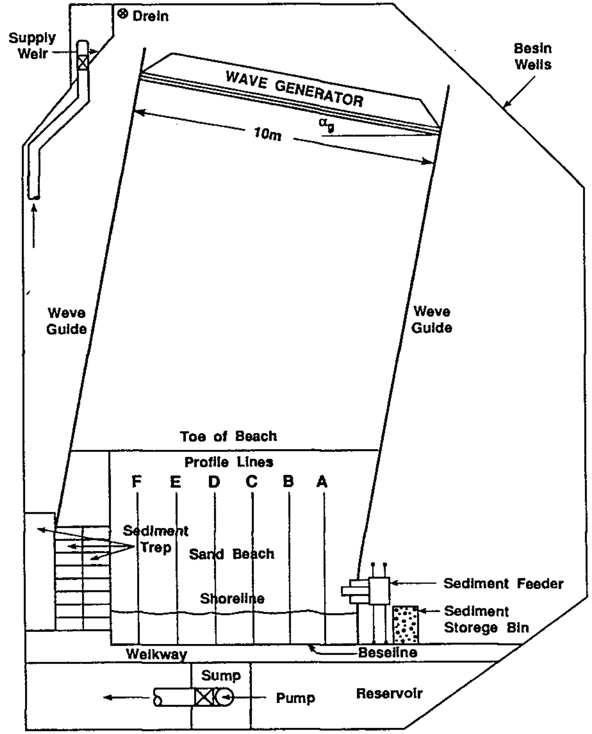

FIGURE 1 WAVE BASIN

waves. Each test was divided into one hour segments. Wave heights, wave angles, longshore current velocity distributions, sediment transport rates and distributions, and beach profiles were measured in an hourly cycle.

Waves were measured at a sampling rate of 10 HZ, offshore and at 15 locations, 0.2 m apart from offshore of the breaker, through the surf zone, into the swash zone. Breaking wave angles were measured for eight of the tests using an overhead video camera (Table 1).

Alongshore current velocities were measured at 0.1 metre intervals across the surf zone using a ducted mini-impeller flow meter.

A sediment trap was located at the downdrift end of the beach but within the lines of the wave guides. It was designed to separate bedload from suspended load and to measure their distributions across the swash and surf zone (Figures 2 and 3). Each trap box extended from above the swash zone to well offshore of the breakpoint and was sub-divided into a number of compartments permit measurement of the distribution of sediment transport across the surf zone.

Templates supporting the trap covers were vertically adjustable to ensure the top of the trap matched the beach profile near the trap. The covers contained slots which extended the full length of the boxes from above the swash zone to offshore of the breakpoint. The slot width (in the sediment transport direction) over the updrift box was adjustable so only bedload was trapped. Any sediment transported past this slot was considered to be suspended load and was trapped through much wider slots over the downdrift boxes.

Sediment was supplied at the updrift end of the beach by a feeder at a rate comparable to the sediment transport rate along the beach. Beach profile measurements and observations of the waves breaking along the beach verified that the beach contours were maintained reasonably parallel by this procedure.

Beach profiles were recorded at the beginning of each test and at the end of each one hour segment using an automatic bed profiler. Profiles were measured at one metre intervals alongshore; depths were recorded at .01 metre intervals offshore. Only the centre 5 m section of the model beach was profiled, resulting in 6 profiles for each one hour segment.

More detail about the experimental procedure may be found in the Kamphuis and Kooistra (1990) and Kamphuis (1991).

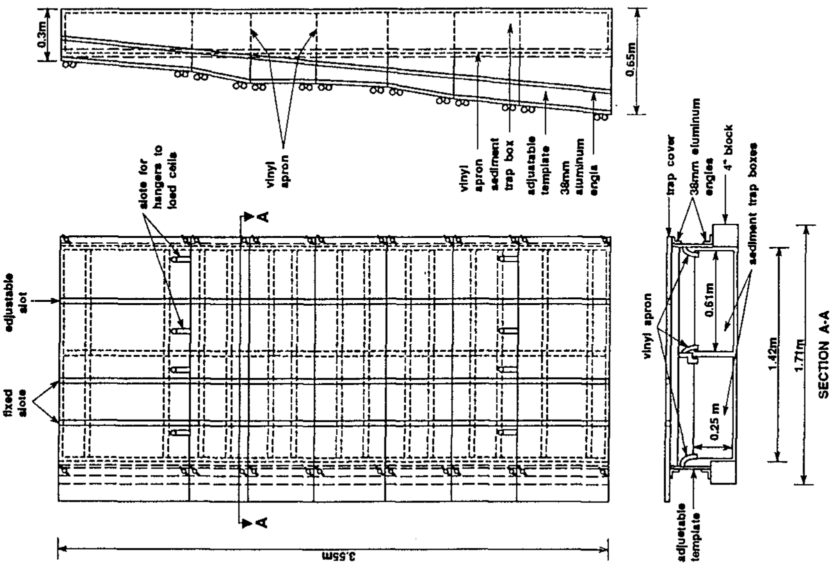

FIGURE 3 SEDIMENT TRAP COVERS AND DETAILS

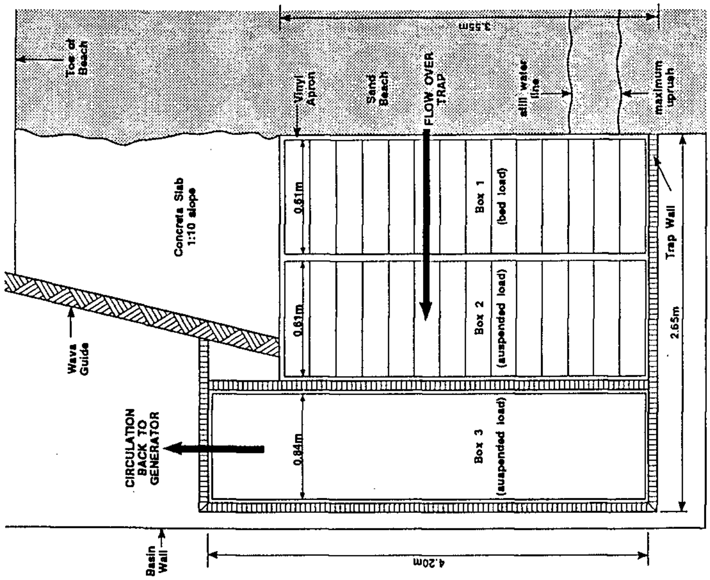

FIGURE 2 SEDIMENT TRAP LAYOUT

3. The Data Analysis

3.1 WAVES

For the irregular waves, the wave period was determined from the peak of the offshore wave spectrum. Significant and rms wave heights were determined at each probe position using a zero crossing analysis. For every hour of the test, wave heights were plotted against probe position as shown in Figure 4. The magnitude and location of the breaking wave height, Hb and Xb respectively, were thus defined and the corresponding values of breaking depth (db) and the distance from the still water line to the breakpoint (λb) were determined from the measured beach profiles. The wave transformation for these tests is discussed in Kamphuis (1990); the wave breaking in Kamphuis (1990a).

3.2 SEDIMENT TRANSPORT

The immersed mass of sediment trapped as bedload, suspended load and total load was measured every 15 minutes and plotted as a function of time as shown in Figure 5. For each one hour segment of the test, the slope of the curve was calculated to determine the sediment transport rate, Q, in kg/s. After approximately three hours of testing, the sediment transport rate approached a steady-state as the beach profile approached equilibrium. At this stage in the test, the trap boxes were pumped completely empty of all sediment and the distribution of sediment transport was measured over the next 3 or 4 hours under equilibrium conditions. A typical plot of the sediment transport distribution is shown in Figure 6.

4. Results

4.1 DIMENSIONAL ANALYSIS

Dimensional analysis for bulk sediment transport rate in the turbulent breaking zone leads to:

$$\frac{Q}{\rho H^3/T} = K \left(\frac{H}{L_o}\right)^a m_b^b \left(\frac{H}{D_{50}}\right)^c \sin^d 2\alpha_b \qquad (1)$$

as demonstrated in Kamphuis (1991). Here a,b,c and d are exponents. Sediment transport is thus a function of wave steepness, beach slope, relative grain size and wave angle and since bulk sediment transport rate is normally assumed to be closely related to alongshore wave thrust, the wave angle term used was ($\sin 2\alpha_b$).

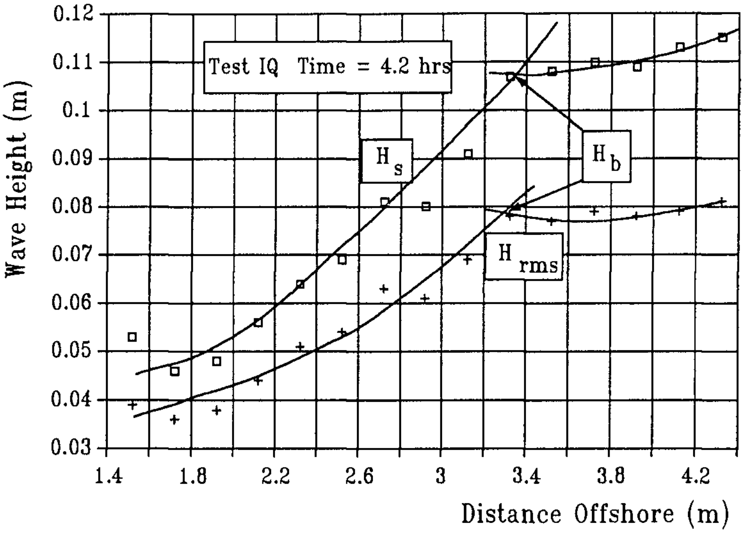

FIGURE 4 BREAKER HEIGHT AND LOCATION

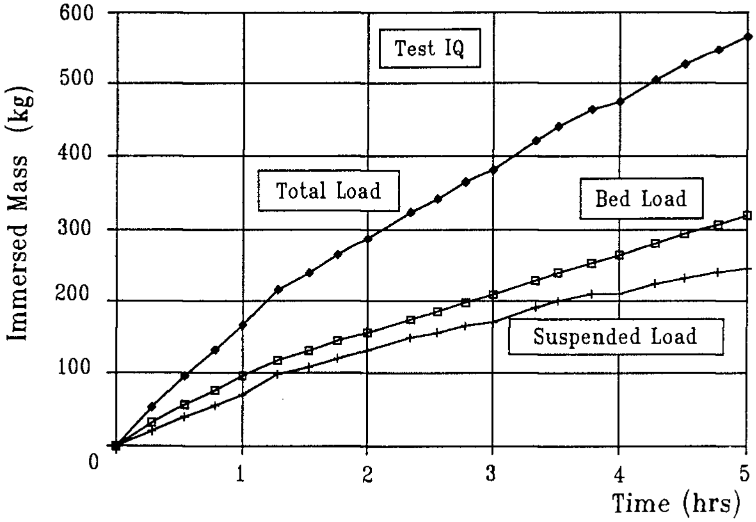

FIGURE 5 MEASURED SEDIMENT TRANSPORT

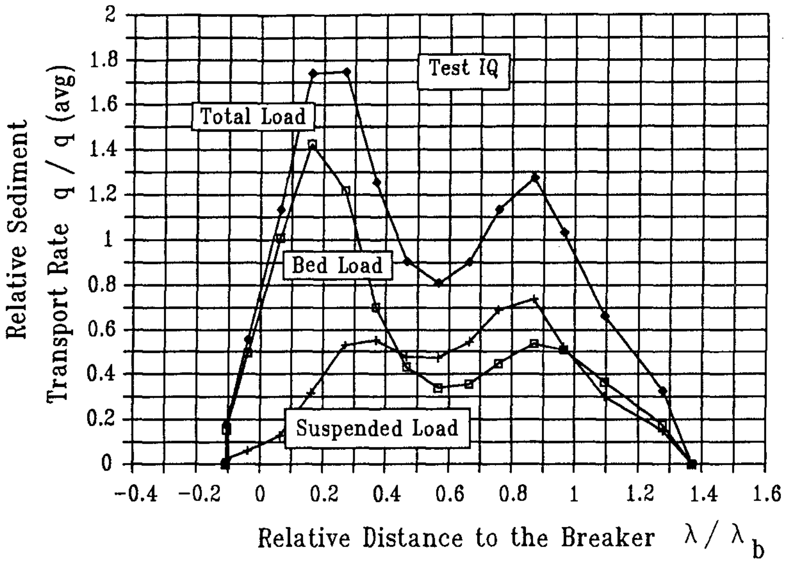

FIGURE 6 SEDIMENT TRANSPORT DISTRIBUTION

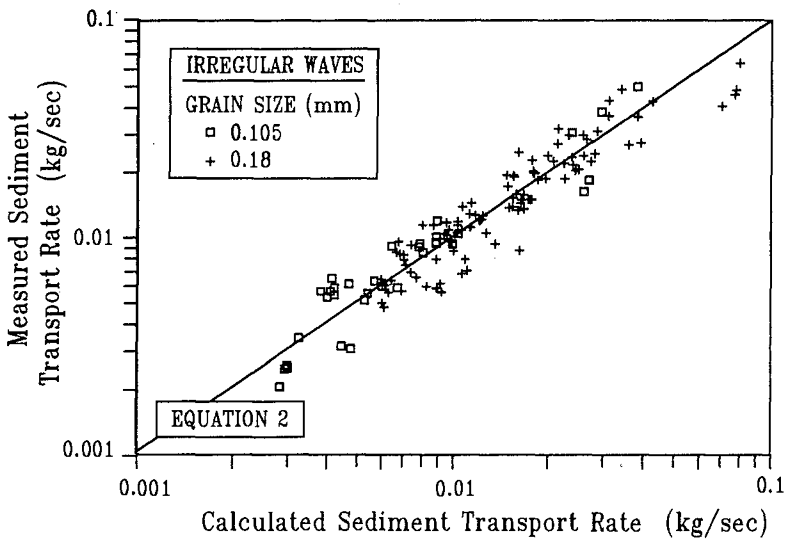

FIGURE 7 IRREGULAR WAVE TESTS

4.2 IRREGULAR WAVE TESTS

Figure 7 shows how:

$$\frac{Q}{\rho H_{sb}^{3}/T_{p}} = 1.3\times10^{-3}\left(\frac{H_{sb}}{L_{op}}\right)^{-1.25} m_{b}^{0.75}\left(\frac{H_{sb}}{D_{50}}\right)^{0.25} \sin^{0.6}(2\alpha_{b}) \qquad (2)$$

fits the experimental data for the irregular waves well. Here Hsb is the breaking significant wave height, Tp is the peak period of the offshore wave spectrum and Lop is the deepwater wave length corresponding to the peak wave period. It is seen that there is no systematic difference between the tests with the two different grain sizes. The standard error of estimate, s(y/x), is 0.10 log cycles, i.e. 95% of the points lie within a factor of ±1.6 times Equation 2.

Sensitivity analysis on the exponents of Equation 2 shows that the actual exponents could vary over the following ranges without materially affecting the result:

$-1.15 < a < -1.30$; $0.6 < b < 0.85$
$0.15 < c < 0.30$; $0.55 < d < 0.6$

A similar analysis using Hrms resulted in:

$$\frac{Q}{\rho H_{rms}^{3}/T_{p}} = 2.6\times10^{-3}\left(\frac{H_{rms}}{L_{op}}\right)^{-1.25} m_{b}^{0.75}\left(\frac{H_{rms}}{D_{50}}\right)^{0.25} \sin^{0.6}(2\alpha_{b}) \qquad (3)$$

with s(y/x) the same as for Equation 2.

Inspection of Equations 2 and 3 shows that Q varies with H^2. If the wave height distribution at breaking approximates a Rayleigh distribution, one would expect the constant in Equation 6 to be twice that in Equation 2. Since this is indeed the case, it would indicate that for bulk sediment transport calculations, a Rayleigh distribution may be assumed for breaking wave heights.

4.3 REGULAR WAVES

Figure 8 shows that if H and T are substituted for Hrms and Tp in Equation 6, the regular waves line up exactly with the irregular wave results. Earlier regular wave results obtained by Readshaw (1978) for much larger grain size (D50 = 0.56 mm) also fit the relationship well. This would indicate that the sediment transport process is indeed closely related to wave energy and that the diameter effect is well simulated by Equation 1.

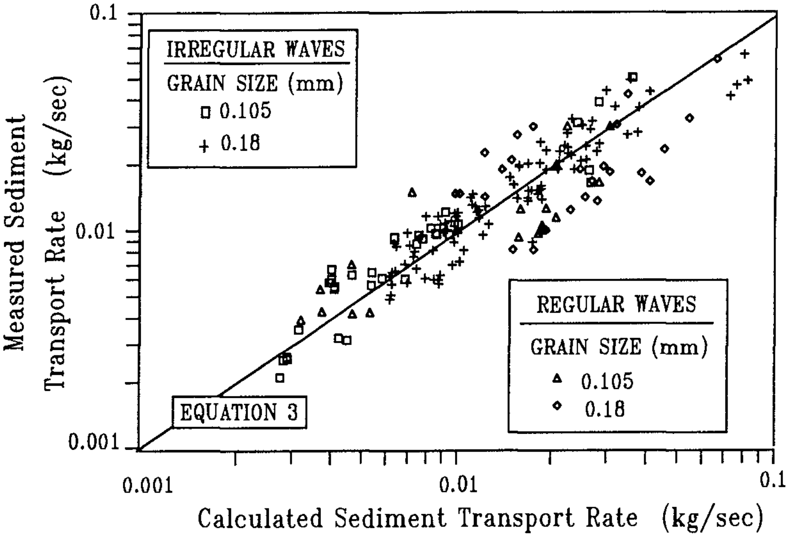

FIGURE 8 REGULAR AND IRREGULAR WAVES

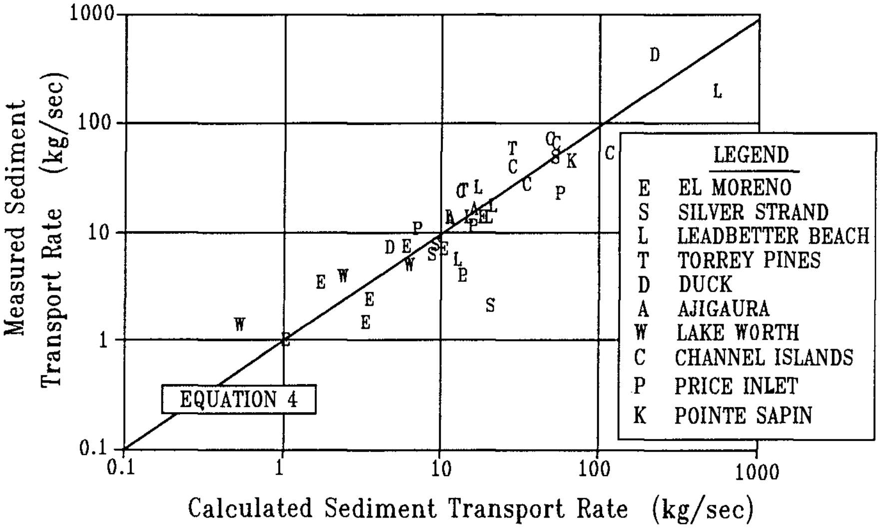

FIGURE 9 FIELD DATA USED

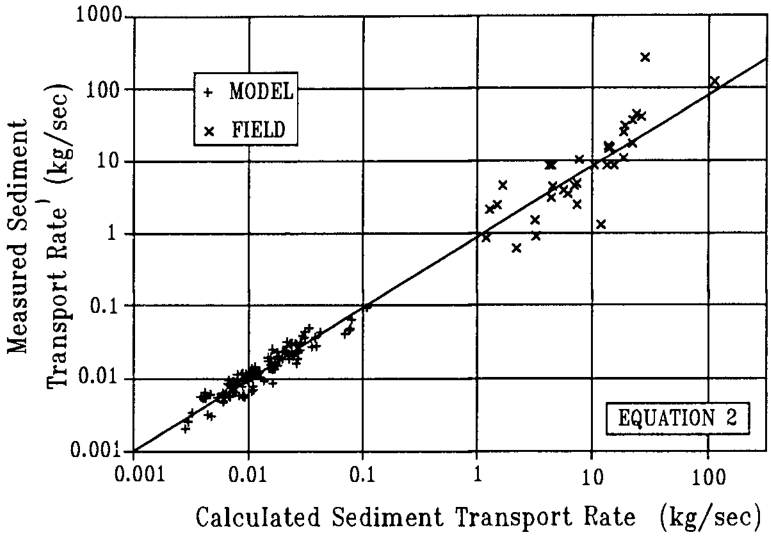

FIGURE 10 MODEL AND FIELD DATA WITH EQUATION 2

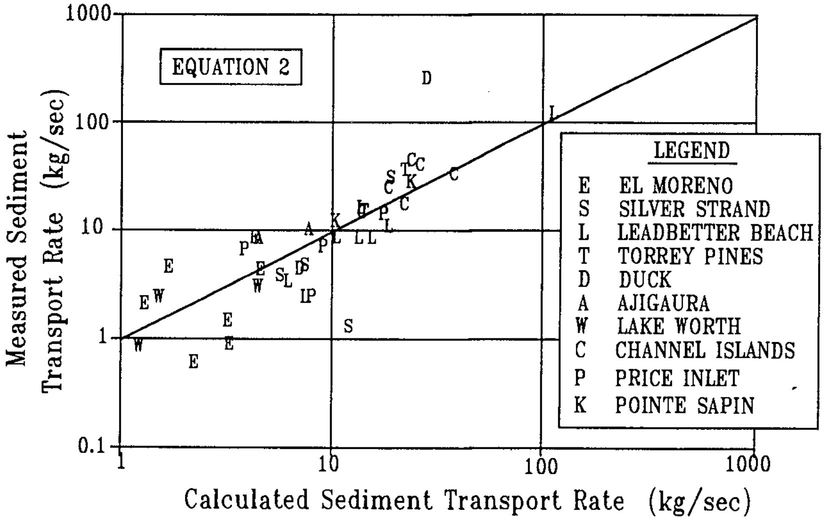

FIGURE 11 FIELD DATA ONLY WITH EQUATION 2

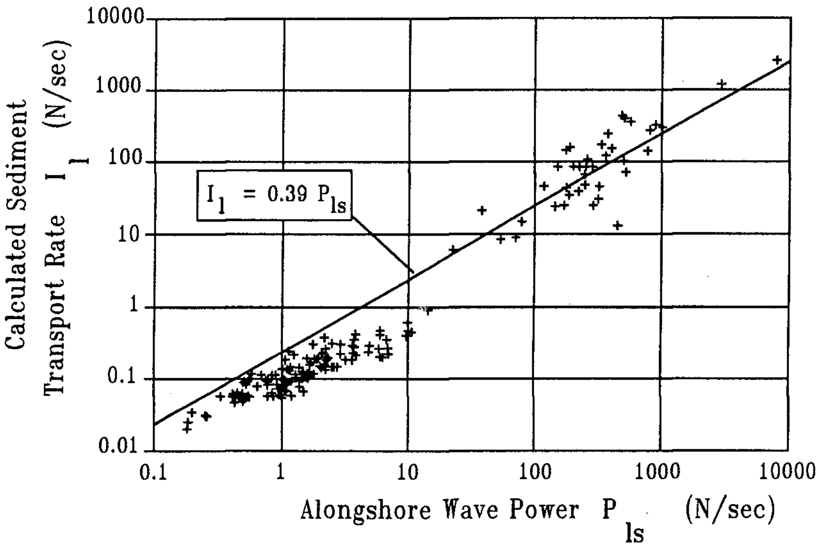

FIGURE 12 CERC EXPRESSION

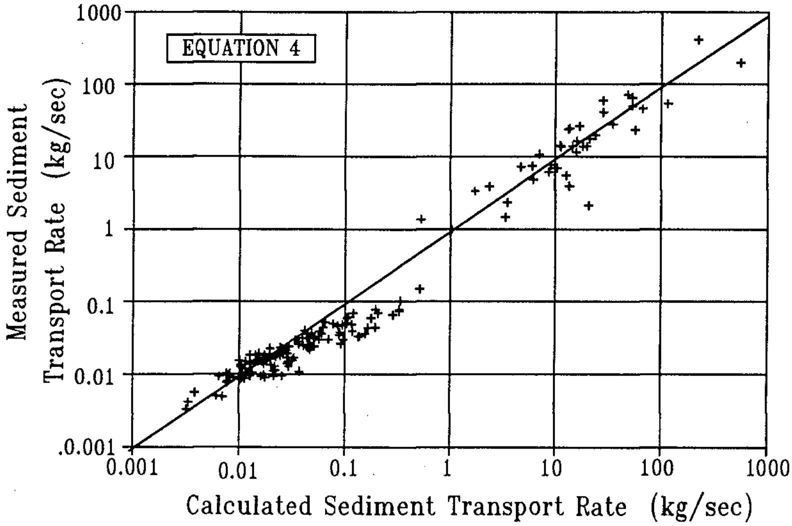

FIGURE 13 MODEL AND FIELD DATA WITH EQUATION 4

4.4 FIELD DATA

The extensive field data set described by Kamphuis et al (1986) is used in the present study. Kamphuis et al (1986) derived a sediment transport expression, based on these field data:

$$\frac{Q}{\rho H_{sb}^{3}/T_p} = 0.6\times10^{-3}\left(\frac{H_{sb}}{L_{op}}\right)^{0.5} m_b^{1.0}\left(\frac{H_{sb}}{D_{50}}\right)^{1.0} \sin\,(2\alpha_b) \quad (4)$$

The field data and their fit to Equation 4 are shown in Figure 9.

Figure 10 shows how Equation 2 fits the irregular wave data and the field data. For the complete data set in Figure 10, s(y/x) is 0.18 log cycles. Figure 11 shows how Equation 2 fits through the field data alone; s(y/x) = 0.33. Clearly Equation 2 represents field conditions as well as model conditions.

To fill the gap between the model and field data, the gravel beach tests of Van Hijum and Pilarczyk (1982) were investigated and Equation 2 appears to be completely robust covering model and field beaches of sand and gravel.

4.5 EARLIER EXPRESSIONS

Figure 12 demonstrates how the well-known CERC expression (Shore Protection Manual - 1984) fits the irregular waves and field data set. It is clear that the CERC expression over-estimates sediment transport for the model tests, particularly for the larger incident wave angles. s(y/x) is 0.60 log cycles for the complete data set and 0.35 for the field data only. If the constant in the CERC expression is changed from 0.39 to 0.12 (the line of best fit), s(y/x) is 0.30 for the complete set and 0.49 for the field data alone.

The same data set is plotted with Equation 4 in Figure 13. It is seen that this expression fits the data better than the CERC expression; s(y/x) = 0.27 for the complete data set and 0.29 for the field data alone.

5. Discussion of Results

Equations 2 and 3 may be reduced to the form:

$$Q = K\,\rho\,(g/2\pi)^{1.25}\;H^{2}\;T^{1.5}\,m^{0.75}\,\bar{D}^{-.25}\;\sin^{0.6}(2\alpha_b) \quad (5)$$

It is seen that the sediment transport rate is proportional to H^2. This exponent of H is smaller than for Equation 4 and the CERC expression. This smaller sensitivity to wave height, corrects a criticism often levelled at the earlier expressions, i.e. that they overpredict sediment transport at high wave heights.

The present expressions are more sensitive to wave period than the earlier expressions.

Sediment transport rate increases with beach slope, a phenomenon noted during the Pointe Sapin field study (Kamphuis et al - 1986). It also shows some inverse variation with grain size. This is as might be expected intuitively, but the small exponent explains the fact that for many years, sediment transport rate expressions have ignored grain size at no great peril.

Sediment transport rate varies with sin $2\alpha b$ to a power smaller than 1. It is clear that sin $2\alpha b$ overestimates the sediment transport at higher incident angles (Figures 12 and 13). Part of the reason is wave-current interaction as discussed by Kraus and Sasaki (1979) and Liu and Dalrymple (1978). But this does not account for all of the observed decrease in sediment transport with wave angle, relative to an expression with sin $2\alpha b$. The present $\sin^{0.6}(2\alpha b)$ is a much more severe wave angle effect than the results given for mean values of longshore currents by Kraus and Sasaki.

8. Conclusions

A bulk sediment transport expression has been presented, based on an extensive, coherent set of laboratory experimental data. The expression correctly predicts sediment transport over a wide range of grain sizes and for field data presented in the literature.

Sediment transport rate is found to be proportional to wave energy since regular wave data and irregular wave data using Hrms form one population.

Sediment transport rate is proportional to H^2, which results in a smaller transport during major storms, as compared to earlier expressions.

Sediment transport rate is a function of beach slope and depends only slightly on grain size. The commonly used wave angle term $\sin 2\alpha b$ over-predicts sediment transport rate.

References

Kamphuis, J.W. (1990), "Wave Transformation", Accepted for publication by Coastal Engineering.
Kamphuis, J.W. (1990a), "Incipient Wave Breaking", Accepted for publication by Coastal Engineering.
Kamphuis, J.W. (1991), "Alongshore Sediment Transport Rate", Submitted to Journal of Waterway, Port, Coastal and Ocean Engineering, (ASCE).
Kamphuis, J.W., Davies, M.H., Nairn, R.B. and Sayao, O.J. (1986), "Calculation of Littoral Sand Transport Rate", Coastal Engineering, Vol. 10, pp. 1-21.
Kamphuis, J.W. and Readshaw, J.S. (1978), "A Model Study of Alongshore Sediment Transport Rate", Proceedings 16th International Conference on Coastal Engineering, Hamburg, pp. 1656-1674.
Kamphuis, J.W. and Kooistra, J. (1990), "Three-Dimensional Mobile Bed Hydraulic Model Studies of Wave Breaking, Circulation and Sediment Transport Processes", Proceedings Canadian Coastal Conference '90, Kingston, Ontario, National Research Council of Canada, Associate Committee on Shorelines (ACOS), pp. 363-386.
Kooistra, J. and Kamphuis J.W. (1984), "Scale Effects in Alongshore Sediment Transport Rates", Canadian Coastal Sediment Study Report No. C2S2-13, National Research Council of Canada, Ottawa, 104 pp.
Kraus, N.C., Isobe, M., Igarashi, H., Sasaki, T. and Horikawa, K. (1982), "Field Experiments on Longshore Sand Transport in the Surf Zone", Proceedings 18th International Conference on Coastal Engineering, Capetown, pp. 969-988.
Kraus, N.C., and Sasaki, T.O. (1979), "Effects of Wave Angle and Lateral Mixing on the Longshore Current", Coastal Engineering in Japan, Vol. 22, 1979, pp. 59-74.
Liu, P.L.-F. and Dalrymple, R.A. (1978), "Bottom Frictional Stresses and Longshore Currents due to waves with Large Angles of Incidence", Journal of Marine Research, Vol. 36, pp. 357-375.
Readshaw, J.S. (1979), "A Model Study of Alongshore Sediment Transport", M.Sc. Thesis, Queen's University, Kingston, 163 pp.
Shore Protection Manual, (1984), 4th edition, Coastal Engineering Research Center, U.S. Army Corps Engineers, Vicksburg.
Van Hijum, E. and Pilarczyk, K.W. (1982), "Equilibrium Profile and Longshore Transport of Coarse Material under Regular and Irregular Wave Attack", Delft Hydraulics Laboratory Publication 274, 107 pp.

Acknowledgements
Financial support for this study was provided by a Strategic Grant (OCEANS) from the Natural Sciences and Engineering Research Council (NSERC).